Large-Scale Characteristics of Tropical Cyclones

WILLIAM M. FRANK

Department of Environmental Sciences, University of Virginia, Charlottesville 22903

(Manuscript received 2 November 1981, in final form 29 January 1982)

ABSTRACT

Rawinsonde composites from the west Pacific and West Indies are used to analyze some of the properties of tropical cyclones and their influences upon larger scale circulations. Composites of storms with different intensities are compared to determine the scales of different circulation features. The radial wind and vertical motion anomalies which occur during the transition from pre-storm convective system to mature tropical cyclone are found to be confined to the inner 6° and 2°, respectively, while the tangential circulation increases at least to the edge of the 15° grid.

Tropical cyclones are found to be net sources of kinetic energy and sinks of relative angular momentum. Of the storms studied, only typhoons made significant contributions to large-scale meridional fluxes of westerly momentum and kinetic energy through a plane 10° north of the storm centers. Fluxes of other quantities were negligible. All of the tropical weather systems were found to be largely thermodynamically self-contained when viewed on a scale of 12° radius.

The wake regions of westerly-moving tropical cyclones are favorable locations for subsequent tropical cyclogenesis while the path areas ahead of the cyclone are generally suppressed for storms exhibiting significant upper level outflow to the southwest.

1. Introduction

Previous research has shown that a number of the structural features and dynamic processes of tropical cyclones appear to extend to large radii (Frank, 1977a,b; Nunez and Gray, 1977; Erickson and Winston, 1972; Black and Anthes, 1971; Vincent and Waterman, 1979), but it has never been clear to what extent the observed large-scale features were predominantly storm or environment. In addition, the relationships between large-scale (~10–15° radius) structure and central core intensity and the roles of tropical cyclones in the general circulation are not well known. In the current study two approaches were used to address the above problems. First, composite analyses of tropical cyclones and cloud clusters in the western North Pacific (WPAC) and West Indies (WI) were compared to determine the horizontal scales of various circulation features, their relationships to the strength of the core circulations and possible roles of tropical cyclones in the general circulation. Second, composites of fixed geographical areas were performed before, during and after the passage of mature tropical cyclones to evaluate the horizontal extent and residual effects of the storms.

2. Methodology

a. Data

The data sets (Table 1) consist of historical rawinsonde data from the stations shown in Figs. 1 and 2. Up to twenty years of data (1956–75) were available for the Pacific stations, and fourteen years of data (1961–74) were used in the Atlantic composites. Three data sets were chosen from each region for the storm comparisons (locations are shown in Figs. 1 and 2). These stratifications were classified by McBride (1981a,b) and McBride and Zehr (1981) and are described in more detail in those papers. Their research focused on the structure from 2–6° radius and did not address system properties at radii greater than 8°. In the present study greater reliance is placed on comparison between the Atlantic data sets since they all exhibit similar mean latitudes, while in the Pacific, the typhoon composite represents a more northerly latitude than do the others.

1) PACIFIC DATA SETS

PN1—Pacific cloud cluster: summertime non-developing Western Pacific cloud clusters. Positions were obtained from ESSA satellite pictures.

PD2—Pacific pretyphoon cloud cluster: positions were obtained from ESSA satellite pictures and by extrapolation from JTWC best tracks. This data set consists of that portion of each storm's track prior to one day before the first reconnaissance aircraft observation.

PD4—Typhoon: positions are from JTWC best tracks. All storm positions from the years 1961–70 such that the central pressure of the storm was less than or equal to 980 mb and such that the latitude

0027-0644/82/060572-15$07.75

TABLE 1. Data sets used in compositing. The 120 B, 120 A, etc., data sets refer to time periods 120 h before and after storm passage, respectively.

Data sets	Estimated maximum winds	Total soundings	Mean latitude (deg N)	Mean longitude (deg)
PD4 Typhoon	≥ 33 m s^{-1}	7778	22	136E
PD2 Developing cluster	10 m s^{-1}	2408	10	153E
PN1 Non-developing cluster	10 m s^{-1}	1986	11	149E
120 B	≥ 33 m s^{-1}	410	18	134E
60 B	≥ 33 m s^{-1}	673	18	136E
Center	≥ 33 m s^{-1}	890	18	136E
60 A	≥ 33 m s^{-1}	748	18	136E
120 A	≥ 33 m s^{-1}	491	18	137E
AD4 Hurricane	≥ 33 m s^{-1}	4796	23	79W
AD2 Depression	15 m s^{-1}	2184	21	75W
AN1 Non-developing cluster	10 m s^{-1}	3176	20	82W
120 B	≥ 33 m s^{-1}	515	20	77W
60 B	≥ 33 m s^{-1}	730	19	75W
Center	≥ 33 m s^{-1}	1009	20	75W
60 A	≥ 33 m s^{-1}	595	20	78W
120 A	≥ 33 m s^{-1}	419	20	75W

was less than 30°N are included. [These are the data analyzed by Frank (1977a,b).]

2) ATLANTIC DATA SETS

AN1—Atlantic cloud clusters: tropical weather systems which subjectively appeared in satellite photographs to have potential for development into tropical storms. If a circulation center for the disturbance was visible, it was defined as the position of the system; otherwise the center of mass of the cloud area was used.

AD2—Atlantic prehurricane depression: positions for this data set are from the official best tracks of the National Hurricane Center (NHC). It represents the depression before it begins any significant intensification.

AD4—Hurricane: official best track positions of the National Hurricane Center for the years 1961–74.

The developing system data sets (PD2 and AD2) differ in intensity with the Atlantic system being somewhat stronger. Directly comparable data sets of good quality (greater than ~2000 soundings) are not available. The developing systems do not include the early stages of all of the mature storms used, but they are considered representative of developing stages.

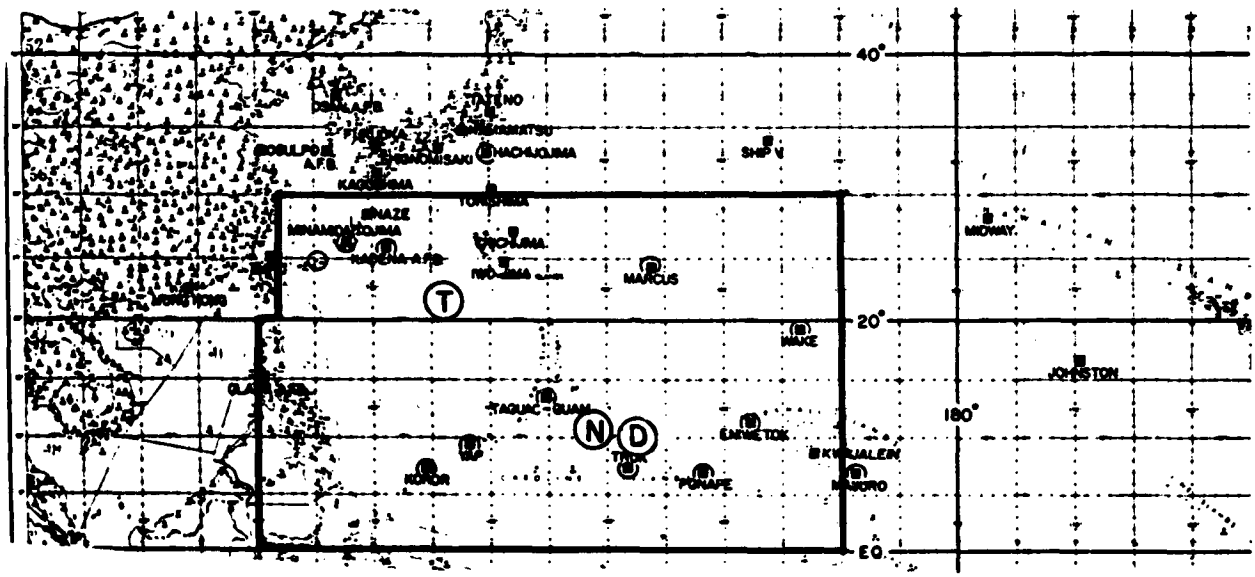

FIG. 1. Western Pacific (WPAC) rawinsonde network. T, D and N show the mean locations for the typhoon, prestorm cloud cluster and non-developing cluster composites.

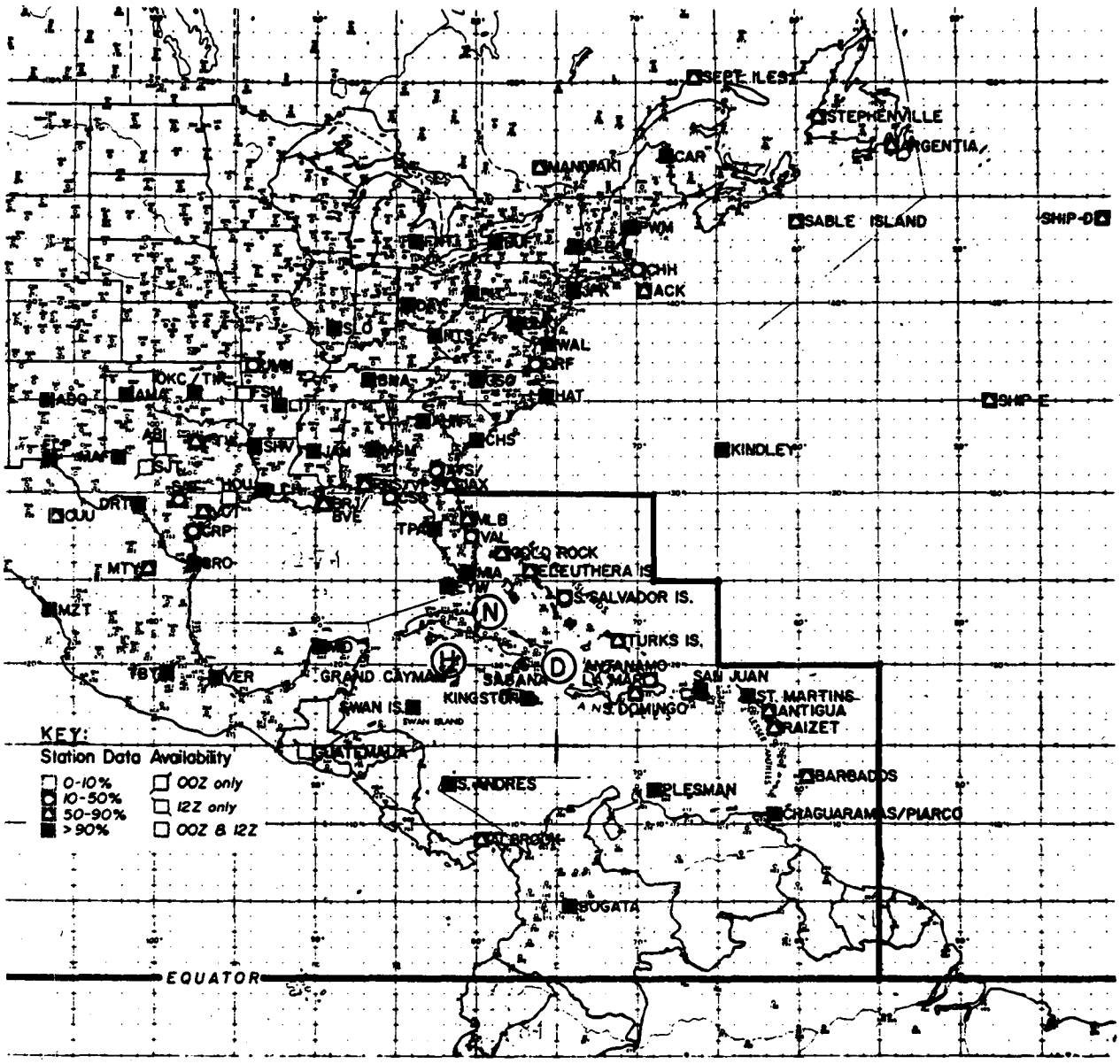

FIG. 2. West Indies (WI) rawinsonde network. H, D and N show the mean locations for the hurricane, developing depression and non-developing cluster composites.

For the study of circulation changes associated with tropical cyclone passage, two other data sets were assembled. Typhoon and hurricane tracks were examined to determine times when mature storms were moving on northwest tracks at a speed such that they were at least 7.5° radius away from the grid center ±48 h from their time of passage. The average tracks and speeds were 289° at 6.9 m s^{-1} (WPAC) and 296° at 5.1 m s^{-1} (WI). Storms which were located over significant land masses, north of 30° latitude (WPAC), north or northwest of the Greater Antilles (WI), or in the South China Sea were eliminated. Storms which had another tropical cyclone within 12° radius of the grid center at any time within ±72 h of storm passage were also eliminated. At ±120 h there were a few typhoons or hurricanes on the compositing grid (less than 10% of the time). They were about equally distributed between the five days before and five days after composites and should have minimal impact on the results. The resulting data sets consisted of 166 observation times for the Pacific and 80 for the Atlantic. These relatively small

samples were sufficient for computation of large-scale features but were not large enough to be stratified into smaller classifications.

b. *Compositing technique*

The specific compositing technique is essentially similar to that developed by Frank (1976, 1977a,b,c) which was based on the earlier method of Williams and Gray (1973) and will be described only briefly. At each observation time a cylindrical grid is placed on the storm center. The grid has eight radial bands extending to 15° radius and subdivided into eight octants with 21 vertical levels ranging from the surface to 50 mb. The 15° maximum radius was selected as the approximate limit for use of a cylindrical grid on a spherical earth. Rawinsonde observations falling in any of the 64 horizontal grid sectors are averaged with other values in the same sector. In this manner it is possible to obtain spatial resolution adequate for quantitative analyses despite extremely sparse data coverage at any one time. Individual features of systems are averaged out, but persistent asymmetries are resolved. Also, certain nonlinear processes such as horizontal fluxes are retained by compositing individual flux values (e.g., $\overline{V,q}$) rather than merely computing fluxes from averaged variables (e.g., $\overline{V},\overline{q}$) where the overbar represents an average over all times and storms. When properly used, compositing has proven to be a successful technique for diagnostic analysis of tropical weather systems (e.g., Reed and Recker, 1971; Williams and Gray, 1973; Shea and Gray, 1973; Reed *et al.*, 1977; Frank, 1977a,b; McBride, 1981a,b).

For the storm comparison composites the grid was always placed with the center of circulation at the center of the grid. However, the storm passage composites employed a stationary grid. At each storm observation time (t_0) the grid was centered on the storm, and data were averaged with data from all of the other centered times. Next, the grid remained fixed on that point while rawinsonde data taken five days earlier ($t_0 - 120$ h) were averaged with data taken five days prior to other storm times, i.e., a composite of a region five days prior to storm passage was obtained. Similar composites were constructed for grids 2.5 days before and 2.5 and five days after the passage of the storm. Storms were typically well off the grid (more than 20° from grid center) at ±120 h.

Meridional fluxes of quantities were calculated from individually averaged values of $v \cdot X$ where X is any variable and v is the meridional wind. Several techniques were tested. The most satisfactory method was found to be computation of the vertically integrated flux across surface–100 mb planes located 10° north and south of the storm latitude. Computation of net meridional fluxes through the x–z (zonal–vertical) plane running through the storm center were deemed less satisfactory due to sensitivity to calculations in the core region where the winds were strongest and least-well sampled. Since the objective was an estimate of the storm's possible role in global fluxes, strong meridional fluxes near the longitude of the core, real or not, were not considered significant unless they were manifest at a distance of 10° latitude north or south of the storm.

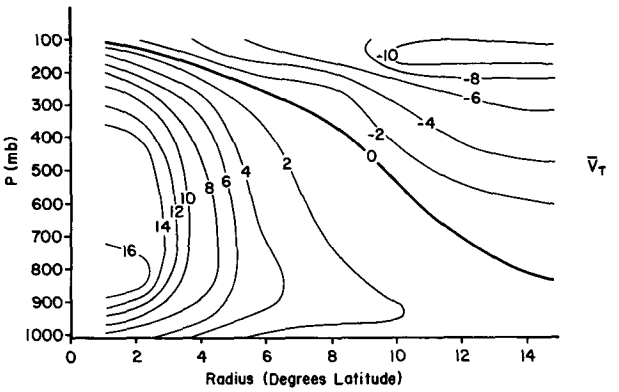

FIG. 3. Tangential wind field for typhoons after the winds of the WPAC developing cloud clusters have been subtracted out (m s^{-1}).

3. Results

a. *Scale of circulations*

Composite studies of typhoon structure (Frank, 1976, 1977a) have shown that the tangential circulation patterns of those storms can be analyzed at least to the edge of the 15° radius compositing grid. The former report presented left–right cross sections (looking downstream along the track) for composites of WPAC tropical cyclones grouped by intensity. Those diagrams indicated that at large radii the circulations were dominated by the upper tropospheric anticyclone and suggested that the intensities of both the cyclone and anticyclone varied in proportion with the central core intensity. These relationships are more clearly documented in Fig. 3 which shows the tangential circulation of a typhoon after the circulation of the pretyphoon cloud cluster has been subtracted out (the core is not analyzed due to insufficient observations). This procedure removes the large-scale circulation along with the pre-storm disturbances. Fig. 4 shows the analogous difference in tangential circulation between mature hurricanes and developing WI tropical depressions. As the systems develop, the tangential wind anomaly is of very large scale. This is consistent with the very large values of the radius of deformation found at low lat-

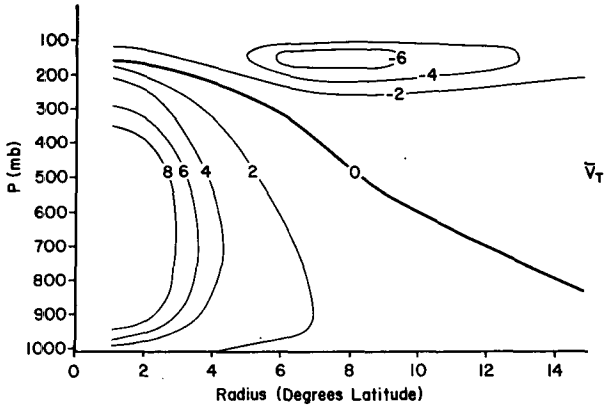

FIG. 4. Tangential wind field for hurricanes minus winds for WI developing depressions (m s^{-1}).

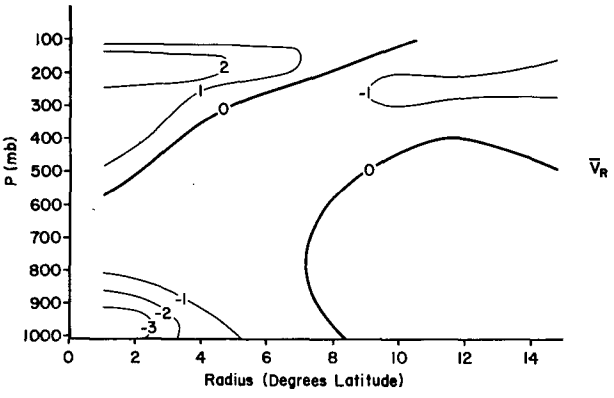

FIG. 6. Radial winds, hurricanes minus WI developing depressions (m s^{-1}).

itudes which imply that the scale of atmospheric response to the storm's core latent heat inputs should be on the order of thousands of kilometers. The observed large-scale changes in V_T are presumably due to radial wind flow sustained typically over several days. Non-developing cloud clusters tend to exhibit lifetimes on the order of one day. The greater V_T anomalies in the Pacific case result from the greater intensity of the Atlantic developing depression compared to that of the Pacific pretyphoon cluster. In addition, typhoons typically develop stronger large-scale circulations than do hurricanes.

Figs. 5 and 6 represent the typhoon–developing cluster and hurricane–developing depression differences with respect to the radial wind fields. The resulting vertical motion anomalies are shown in Figs. 7–8. The patterns are similar in both regions. The increases in radial circulation which occur during tropical cyclone intensification are restricted to the inner 6° of radius, and there is some suggestion that the radial mass flux on larger scales (~12° radius) slightly decreases. At the mature stage the tangential wind patterns are sufficiently strong so that horizontal fluxes of angular momentum by the radial flow essentially balance the effects on V_T of the Coriolis parameter acting on the radial flow (Frank, 1977b). The upward vertical motion anomaly is found only within ~2° of the center with slightly increased mean subsidence indicated at larger radii as the systems strengthen. Numerical simulations of tropical cyclones generally show concentration of the upward motion inside ~100 km radius (e.g., Ooyama, 1969; Rosenthal, 1970). Rodgers and Adler (1981) examined satellite microwave data from 21 Western Pacific tropical cyclones and found that virtually all of the storm rainfall occurred within 300–400 km radius.

The basic similarities of the radial winds and differences between the tangential winds at large radii are evident in Figs. 9–10 which show vertical profiles of these quantities at 12° radius (smoothed from 9–15°). Viewed from the perspective of this large scale, the major change associated with tropical cyclone intensification is the strengthening of the upper level anticyclone. Differences in thermodynamic variables are insignificant at this radius and are not shown.

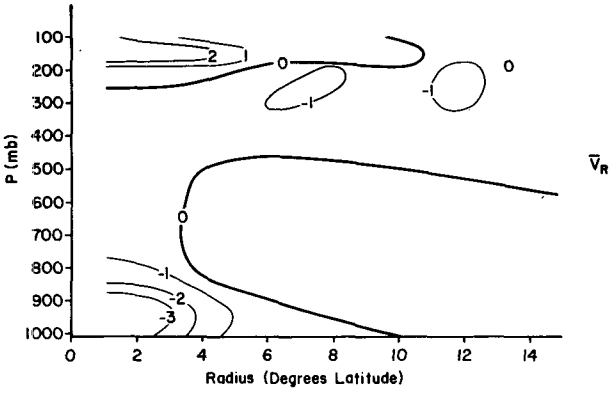

FIG. 5. Radial winds, typhoon minus WPAC developing cluster (m s^{-1}).

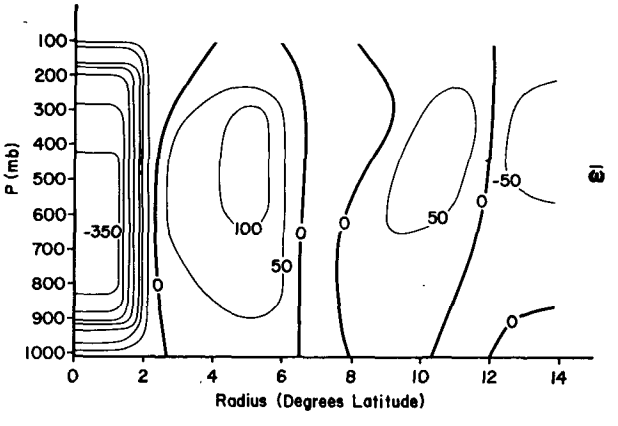

FIG. 7. Vertical motion, typhoons minus WPAC developing clusters (mb day^{-1}).

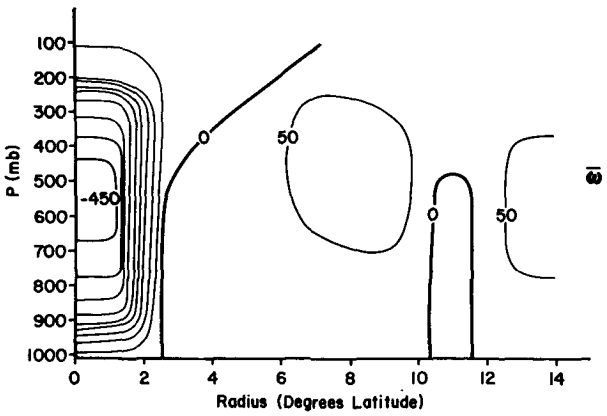

FIG. 8. Vertical motion, hurricanes minus WI developing depressions (mb day^{-1}).

b. *Tropical cyclones as large-scale energy and momentum sources*

The six data sets used in the comparison studies were examined to determine whether the systems acted as large-scale sources or sinks of various quantities. Radial fluxes of kinetic energy (KE), relative angular momentum (m), moist static energy (h), dry static energy (s) and water vapor (q) were computed at each level (using all available 0000 and 1200 GMT soundings) and vertically integrated from sea level to 100 mb. Radial mass fluxes were mass balanced. The vertically integrated fluxes between 9 and 15° radius were smoothed to produce mean radial fluxes at 12° radius, and mean flux divergences were calculated for the 0–12° radius in the manner of Eq. (1) (Table 2):

$$\int_{P_0}^{100} \nabla \cdot \mathbf{v}h \frac{dp}{g} = \frac{2}{gr} \int_{P_0}^{100} \overline{V_R h}\, dp, \qquad (1)$$

where g is the gravitational constant, P_0 is surface pressure in millibars, r = 12° radius (1.33×10^6 m). In Eq. (1) the moist static energy is defined

$$h = s + Lq = c_pT + gz + Lq \qquad (2)$$

where L is the latent heat of condensation. McBride (1981b) presented budget analyses of these systems for the inner 0–6° radius regions.

The last four columns of Table 2 show that large-scale radial fluxes of h, s and q are relatively small and apparently unrelated to core intensity. The systems converge moisture and diverge dry static energy due to their low-level mass convergence and upper-level mass divergence. The result is a small net export of moist static energy on the order of 40–90 W m^{-2} (radiational cooling is ~130 W m^{-2} equivalent to −1.2°C day^{-1}). The lack of a clear relationship between core strength and net exports of h, s, or q at 12° radius reflects the relatively small scale of the radial wind perturbation associated with storm intensification. McBride's (1981b) analyses of fluxes at inner radii showed increasing exports of h and s and imports of q at 4° radius with increasing storm intensity.

The developing depression and mature tropical cyclones act as sinks of relative angular momentum (due to their broad cyclonic circulations at the surface) while the cloud clusters do not. The import of momentum at large radii in typhoons is concentrated in the upper troposphere (Frank, 1977b) and is integrally related with the anticyclonic outflow channels which tend to form as the storms develop.

Kinetic energy export is ≥0 at 12° radius for all of the systems with the typhoon exhibiting the largest value. Frank (1977b) showed that kinetic energy fluxes at 12° radius in mature hurricanes and typhoons are concentrated in the upper troposphere. McBride's (1981b) results for 6° radius are similar. Black and Anthes (1971) have also shown the strong momentum imports and kinetic energy exports at

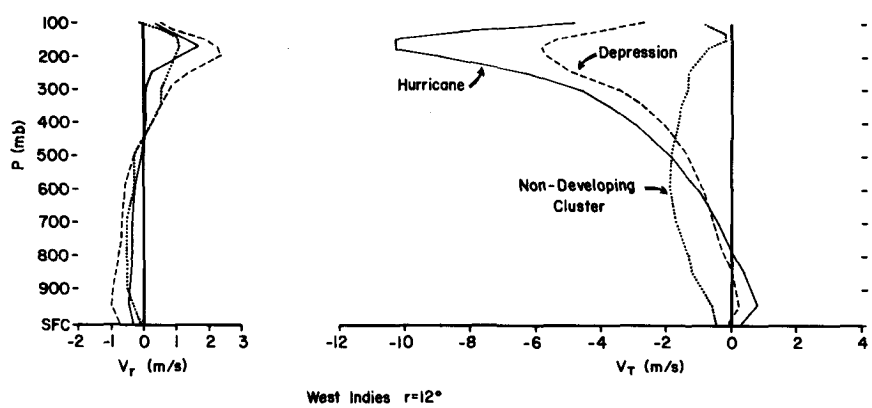

FIG. 9. Radial and tangential winds at 12° radius around hurricanes (solid), developing depressions (dashed) and non-developing clusters (dotted). Winds are smoothed from 9 to 15° (m s^{-1}).

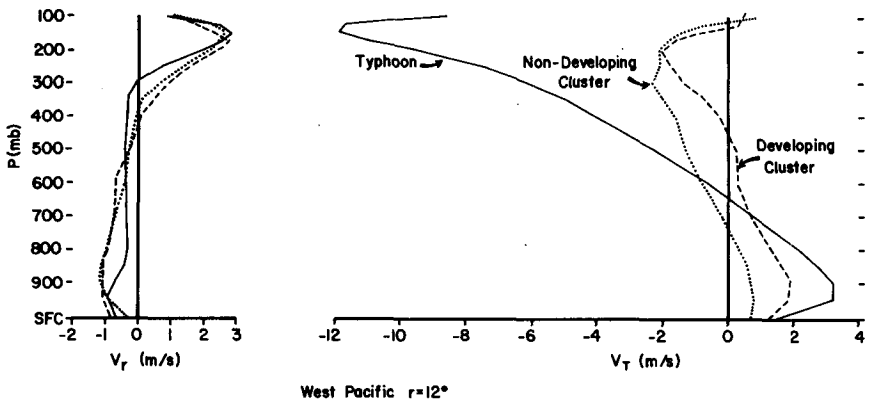

FIG. 10. As in Fig. 15 for typhoons (solid), developing clusters (dashed) and non-developing clusters (dotted).

large radii in the upper levels of both a group of hurricanes and composite storms. Edmon and Vincent (1979) analyzed kinetic energy budgets of a moving 10 × 10° square (~5° radius) centered on Hurricane Carmen (1974). They found negligible exports of kinetic energy. This is not necessarily inconsistent since Frank (1977a) showed that mean kinetic energy exports from typhoons increase greatly with radius and are typically near zero between 3 and 4° radius. Palmén (1958) showed strong exports of kinetic energy from Hurricane Hazel at large radii during the storm's over-land transformation into an extratropical storm.

From the flux computations of Table 2 it may be concluded that tropical cyclones do not influence heat and moisture balances on a scale larger than 12° radius to any different degree than do cloud clusters. However, the more developed storms do tend to act as sinks of angular momentum from and sources of kinetic energy to larger scales.

c. *Meridional fluxes*

The roles of tropical weather systems as large-scale sources or sinks of energy and momentum were discussed above. It is also of interest to determine whether the systems contribute to global meridional transports of these quantities. As previously mentioned, the net fluxes through x–z (zonal-vertical) planes located 10° north and south of the system center were computed. The planes extended from the surface to 100 mb, and their effective length in the x direction was ~28° centered on the storm longitude. Values from the cylindrical grid were subjectively analyzed to yield the estimated mean fluxes ±10° from the center. Results are shown in Table 3 for fluxes of kinetic energy, westerly momentum (u), latent heat (Lq) and moist static energy. Also shown for scaling purposes are mean fluxes computed by assuming a constant meridional wind of 1 m s^{-1} and mean vertically integrated values of the transported quantities taken from the West Indies non-developing cluster. These latter fluxes are included to allow comparison of the composite fluxes with transports resulting simply from a mean meridional mass flux at the storm longitude.

The results of Table 3 show that meridional fluxes of all of the quantities are rather small and poorly related to system intensity with the exception of some of the WPAC typhoon fluxes. Typhoons show large northward transports of KE and u, 10° north of the storm center. These fluxes are almost entirely confined to the upper troposphere and are maximum near 200 mb. Erickson and Winston (1972) have shown that 300 mb westerlies over the North Pacific increased for several days following cases when the long cloud bands associated with the upper level northeast outflow channels of WPAC typhoons ex-

TABLE 2. Flux divergences (0–12°).

	Kinetic energy (W m^{-2})	Angular momentum (×10^5 J m^{-2})	h (W m^{-2})	s (W m^{-2})	Lq (W m^{-2})	q (cm day^{-1})
Hurricane	1.4	−0.8	44	91	−47	−0.16
Developing depression	1.9	−1.6	61	178	−117	−0.40
Non-developing cluster	0.0	0.3	66	98	−32	−0.11
Typhoon	4.1	−2.2	88	162	−74	−0.25
Developing cluster	0.7	0.0	49	204	−155	−0.54
Non-developing cluster	1.3	0.2	39	186	−147	−0.51

TABLE 3. Poleward fluxes through x–z planes (averaged surface to 100 mb) located 10°N and 10°S of the system center. Also shown are hypothetical fluxes for a uniform $\bar{v} = 1$ m s^{-1} and mean values of $V^2/2$, u, Lq and h for the West Indies non-developing depression.

	$v\frac{1}{2}\overline{V^2}$ (m J s^{-1}kg^{-1})		$\overline{vu}$ (m^{2}s^{-2})		$\overline{vLq} \times 10^3$ (m J s^{-1}kg^{-1})		$\overline{vh}$ (m-J s^{-1}kg^{-1})	
	10°N	10°S	10°N	10°S	10°N	10°S	10°N	10°S
Hurricane	−74	−112	0	5	6	11	−149	−115
Developing depression	242	−37	18	−1	7	13	177	−76
Non-developing cluster	−65	−69	−1	1	10	5	−66	−82
Typhoon	1726	−121	55	17	19	22	748	44
Developing cluster	−2	−45	5	4	7	6	−66	3
Non-developing cluster	−68	−106	7	11	12	11	56	−60
Mean flux for $\bar{v} = 1$ m s^{-1}	33		3		13		342	

tended into the westerlies. The poleward kinetic energy flux by typhoons in Table 3 is sufficient to increase the surface-100 mb kinetic energy of the 10° belt between 30 and 40°N by 11 m^2 s^{-2} day^{-1} (generation of 1.2 W m^{-2}) or the 100–300 mb layer of that belt by 51 m^2 s^{-2} day^{-1} (~5.5 W m^{-2}) neglecting any corresponding export elsewhere. The typhoon momentum flux, if realized as an increase in momentum within the same 10° band, would increase the westerly flow by about 0.3–0.4 m s^{-1} day^{-1} (~1.6 m s^{-1} day^{-1} for the 100–300 mb layer). These values are of the same order as results of Erickson and Winston (1972) which showed a mean $\partial KE/\partial t$ of the 850–200 mb layer for the Northern Hemisphere (20–90°N) of ~2.8 m^2 s^{-2} day^{-1} (or 0.2 W m^{-2}) for 4 days following the formation of a strong northeast outflow band. Their area is about four times larger than the 20–30° band.

It is interesting that WI hurricanes do not show significant meridional fluxes of KE or u 10°N or S of their centers. Since these storms do export net kinetic energy (Table 2), their export must be contained within the zonal band extending ±10° from the center. [Individual values of $u \cdot$KE were not included in the composites, and since large-scale kinetic energy fluxes in tropical cyclones are largely eddy fluxes (Frank, 1977b) the zonal fluxes of kinetic energy could not be calculated.] The net exports of KE at 12° radius by typhoons and hurricanes (flux divergences of 4.1 and 1.4 W m^{-2}, respectively) are sufficient to increase the tropospheric kinetic energy in the 10–30°N band at rates of 0.27 W m^{-2} and 0.09 W m^{-2} per storm. The above calculations do not consider possible storm-related generation of KE at radii greater than 12° radius. For comparison, the dissipation of KE due to surface friction in a region where $V_0 = 10$ m s^{-1} would be ~1.65 W m^{-2}. There are ~80 fully developed tropical cyclones per year (Gray, 1975). Their lifetimes are variable but are of the approximate order of one week. Therefore, averaged over the globe there are on the order of 1–2 active tropical cyclones per day although they are highly seasonal (Gray, 1975) and often several of them occur simultaneously (Gray, 1978). It is clear that they do not dominate the annual kinetic energy budget in the lower latitudes, but they may well be significant on shorter time and space scales—an area which deserves future study. Gray (1978) estimated that tropical cyclone KE generation balances ~2% of the annual global kinetic energy dissipation outside the cyclone areas and may balance as much as 20–30% of the kinetic energy dissipation of the Northern Hemisphere during 10–20 day periods when many storms are present.

d. Storm passage analyses

Fixed grid locations were analyzed with a mature typhoon or hurricane at the center ($t = t_0$) and at $t = t_0 \pm 60$ h and $t = t_0 \pm 120$ h. Since the screening criteria required that the storm be at full tropical cyclone strength (maximum winds ≥ 65 knots) at all analysis times, the number of available cases decreased with increasing time interval before or after passage. Several days prior to storm passage a storm often had not reached maturity, while after passage the storm eventually weakened or made landfall. At ±120 h the number of soundings in the data sets were reduced to ~50% of the t_0 composites. Further extensions in time were not feasible.

Fig. 11 shows time series of vertically integrated (surface–100 mb) values of h, s, Lq and V^2 (=2 KE) for 1–7°, 7–13°, and 1–13° radius areas of the grid for hurricane passages. As expected, all of these quantities exhibit maxima in the 1–7° area when the storm is centered on the grid at t_0. Comparison of before and after composites at ±60 h and ±120 h shows relatively small changes in h, Lq and s. Results are similiar for typhoons (not shown) although there is some tendency for the wake region of typhoons to exhibit slightly higher h and Lq values than does the area in the path of the oncoming storm. For both WI and WPAC storms there are significant increases in the total grid kinetic energy as the storms pass. The

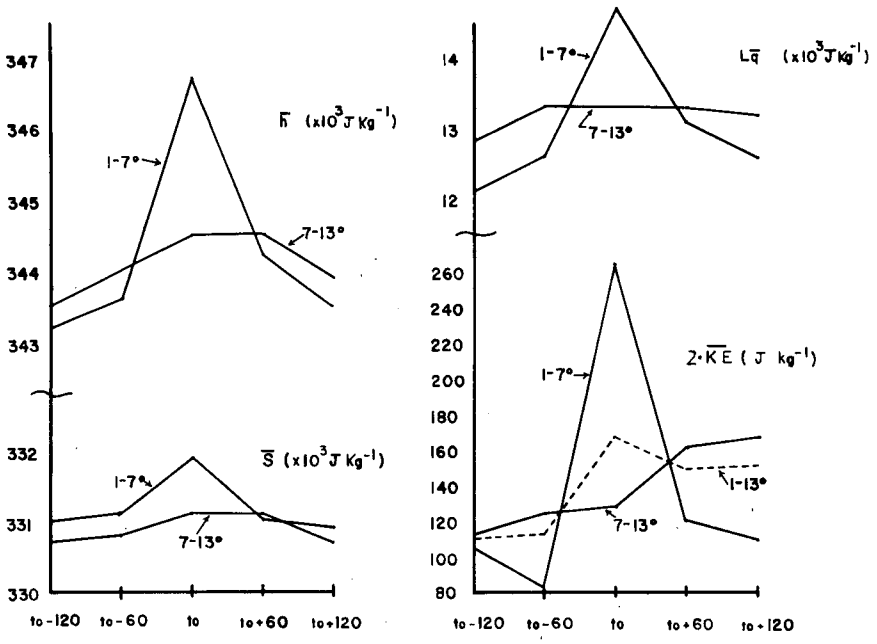

FIG. 11. Time series of moist static energy (h), dry static energy (s), latent heat (Lq) and V^2 = 2 × kinetic energy from 120 h before typhoon passage (t_0 − 120) until 120 h after passage (t_0 + 120). Values are averaged over the 1–7°, 7–13° or 1–13° radius areas.

storms are associated with an increase in the wind speed over a 10-day interval. The values in Fig. 11 can be used to estimate the storage terms ($\partial/\partial t$) in Eulerian budget analyses.

It must be noted that the undisturbed environments of the WI and WPAC regions differ. The WI storms tend to be located north of the easterly trade wind maximum where there is weak negative vorticity and subsidence through the middle and lower troposphere. The WPAC storms are most often found south of the trade wind maximum in a region of mean positive low level vorticity and upward vertical motion. It is also important to examine the differences between the mean upper level structures of hurricanes and typhoons (Fig. 12a–d). Parts a and b of this figure are streamline and isotach analyses of the layers of maximum divergence from McBride (1979) while c and d are plane views of the radial winds from Frank (1976) and Nunez and Gray (1977). The typhoon typically has two strong outflow channels to the northeast and southwest which are undiminished at the maximum composited radius (15°). In contrast the composite hurricane has only a single strong outflow channel located northeast of the storm center which decreases in intensity beyond ~4–6° radius. Note also that the wind speeds at the northeast edge of the grids are stronger in the typhoon and that the hurricane winds in that sector are curving towards the southeast. Black and Anthes (1971) studied outflow from a group of hurricane cases as well as in a composite hurricane (Miller, 1958) and a composite typhoon. They found that tropical cyclone outflow is highly asymmetrical with wavenumber two dominating the mean typhoon outflow at large radii and wavenumber one generally more important in hurricanes.

Figs. 13–14 show time–height cross sections of the 12° radius (smoothed 9–15°) tangential winds for passing typhoons and hurricanes. Both composites show low level cyclonic and upper level anticyclonic maxima at the time of storm passage with the anticyclone being the dominant feature, as previously mentioned. The typhoon composite shows significantly stronger anticyclonic flow near 200 mb both before and after the storm passage than do climatological studies (e.g., Newell *et al.*, 1972) or the composites of weaker systems. This appears to reflect the presence of the storm outflow channels which, in the mean, must extend well beyond the 15° limit of the grid. The typhoons are moving on a mean track of 289° at 6.9 m s^{-1}. Therefore, 60 and 120 h prior to storm passage the southwest outflow maximum (easterly winds) would lie toward the southern edge of the grid, producing anticyclonic shear, while in the wake of the storm the northeast outflow (westerly winds) would lie toward the northern edge, also producing anticyclonic shear. (The systems are usually near the edge of the 15° grid at ±60 h and more than 20° from the center at ±120 h.) The northeast cloud bands of typhoons composited by Erickson and

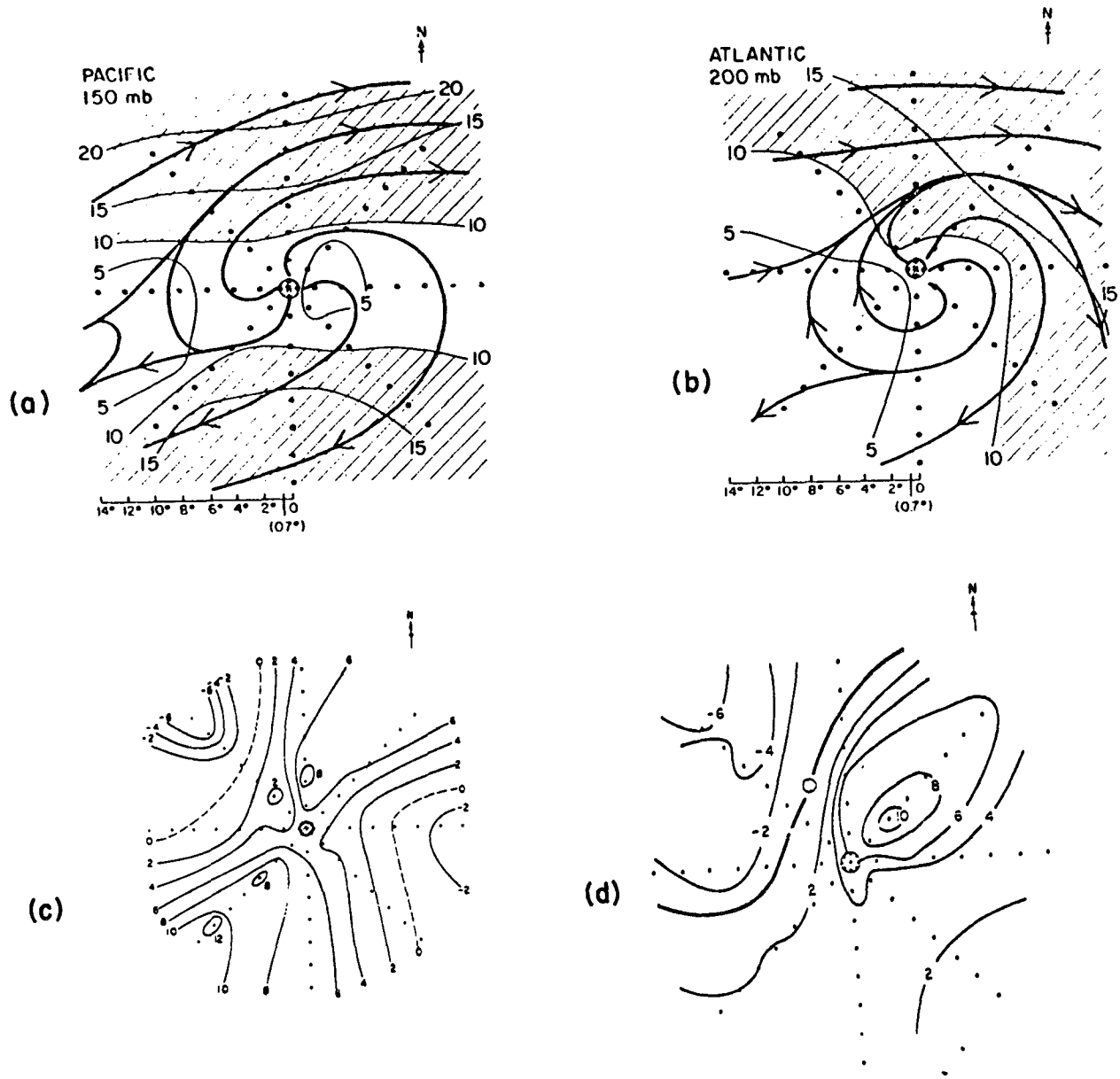

FIG. 12. (a) Streamline and isotach (m s^{-1}) analysis for WPAC typhoons at 150 mb (McBride, 1979). (b) Streamlines and isotachs for WI hurricanes at 200 mb (McBride, 1979). (c) Radial winds (m s^{-1}, positive outward) at 150 mb for WPAC typhoons (Frank, 1977a). (d) Radial winds at 150 mb for WI hurricanes (Nunez and Gray, 1977).

Winston (1972) all extended to distances greater than 20°. The hurricanes show a strong anticyclonic anomaly only at t_0 and t_0 + 60 h (after storm passage). Tangential flow is relatively undisturbed 60 and 120 h before and 120 h after hurricane passage, reflecting the single outflow and smaller circulation patterns of hurricanes.

Figs. 15–16 show the time–height cross sections of the radial wind fields. The typhoon shows suppressed upper-level divergence for the five days prior to storm passage and somewhat enhanced flow afterwards. Satellite photos often show large regions with little convection northwest of typhoons. Vincent and Waterman (1979) showed an area of low middle-level humidities, suggestive of deep subsidence northwest of the westerly-moving Hurricane Carmen (1974). Frank (1977) showed low middle-level relative humidities in the northwest sectors of his typhoon composites, and subsequent kinematic analysis of the composite data indicates weak convergence

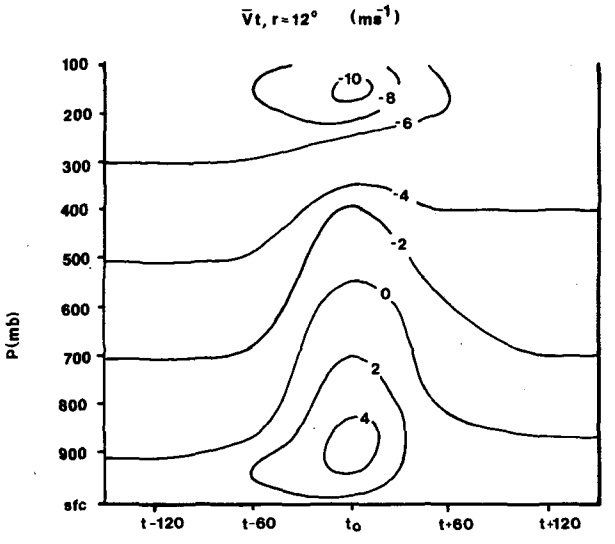

FIG. 13. Tangential winds (m s^{-1}) at 12° radius (smoothed 9–15°) during the passage of typhoons. The time scale runs from five days prior to storm passage (t_0 − 120 h) through five days after passage (t_0 + 120 h).

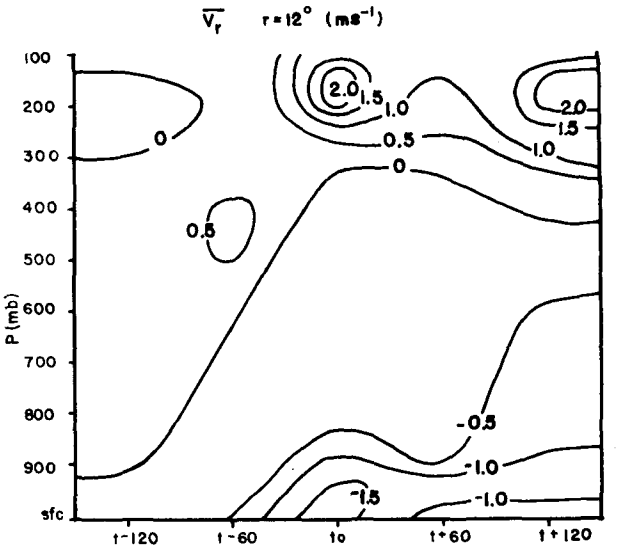

FIG. 15. As in Fig. 13, except for radial winds of typhoons.

between 10 and 14° radius (order 1–3 × 10^{-6} s^{-1}) in the northwest quadrant of the upper-level outflow layer. The hurricane case shows relatively undisturbed (weakly suppressed) conditions 60–120 h before and 120 h after passage with enhanced low-level convergence and upper-level divergence only evident at t_0 and in the wake at t_0 + 60 h. For both the WI and WPAC storms the "enhanced" wake regions exhibit divergences of the same order as do the storms themselves (t_0) and hence as do prestorm developing systems (e.g., Figs. 9 and 10).

e. *Effects on tropical cyclogenesis*

It is clear that the storms influence circulations over large areas—certainly beyond 15° radius in the case of typhoons. This raises the question of whether storms may act to enhance or suppress the formation of other tropical cyclones. Shapiro (1977) suggests that the transformation from an ordinary tropical disturbance to a developing tropical cyclone occurs when the system moves into a favorable large-scale environment. McBride and Zehr (1981) studied the differences between developing and non-developing systems and found that the best indicator of storm development was the vertical gradient of cyclonic shear measured between 200 and 900 mb at ~6° radius. When viewed on a larger scale, their composites suggested that genesis or intensification would occur when there were strong north–south gradients of vertical shear of the zonal wind and the system was located on the zero shear line between regions of positive and negative shear. (Similar results were

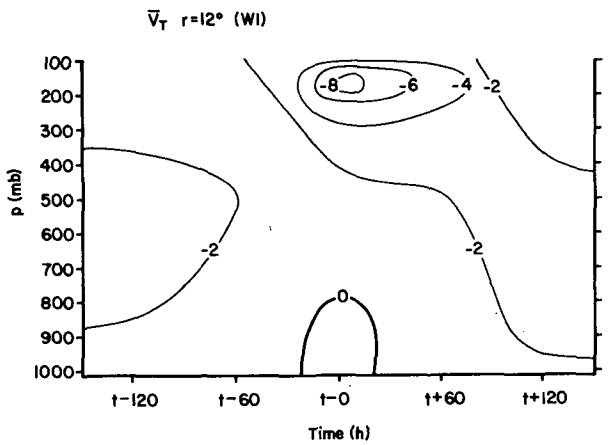

FIG. 14. As in Fig. 13, except for hurricanes.

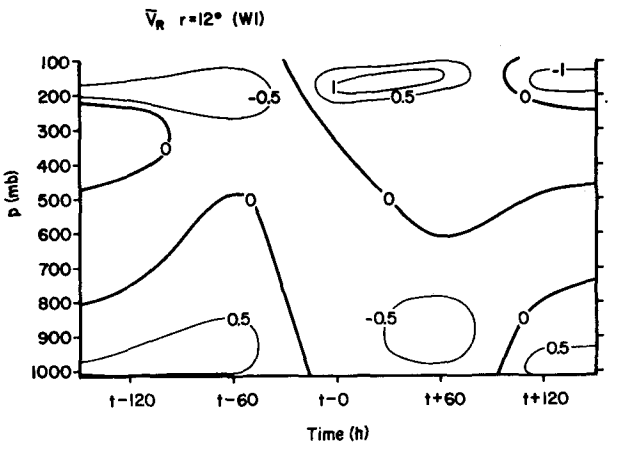

FIG. 16. As in Fig. 13, except for radial winds of hurricanes.

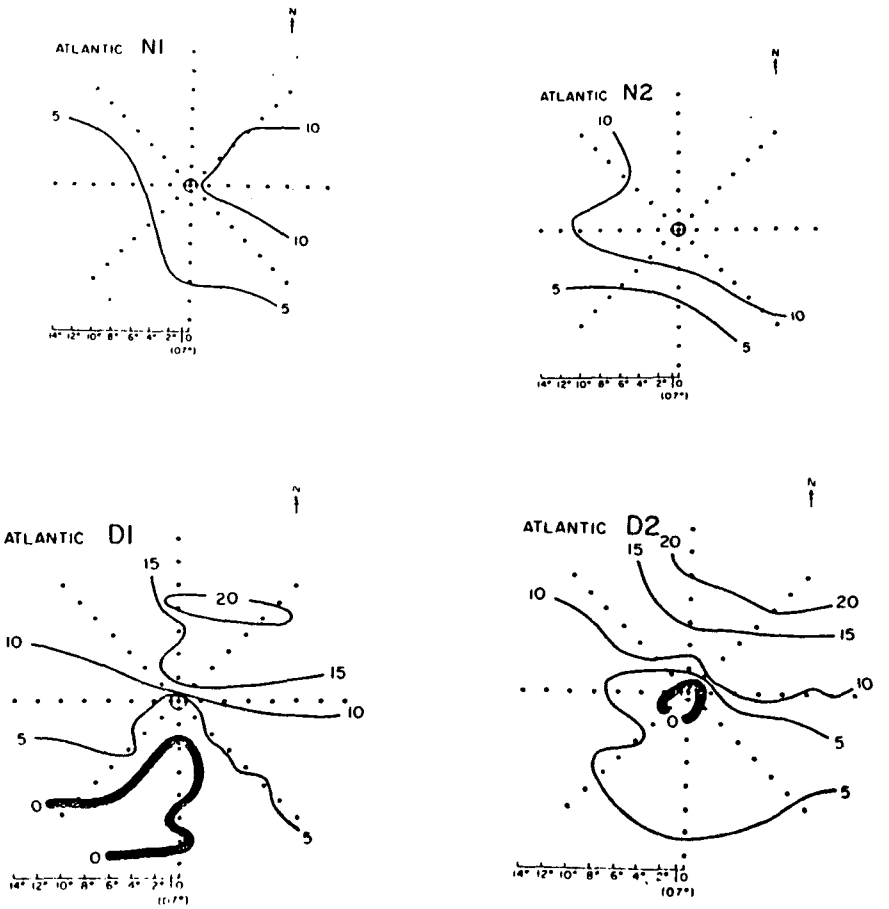

FIG. 17. Vertical shear of the zonal wind (U at 200 mb minus U at 900 mb) for WI non-developing clusters (N1, N2), pre-hurricane clusters (D1) and developing depressions (D2) from McBride and Zehr (1981) (m s^{-1}).

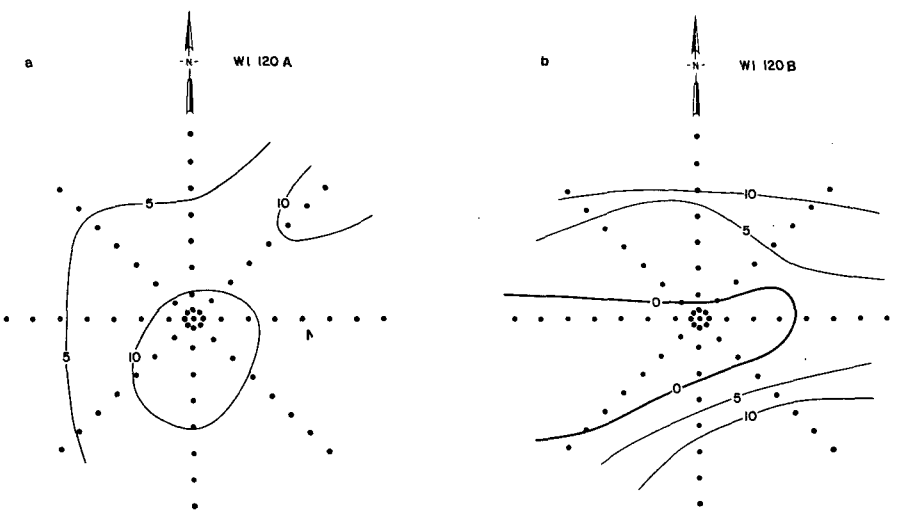

FIG. 18. Plan view of vertical shear of the zonal wind (U at 200 mb minus U at 900 mb) 120 h prior to the passage of a hurricane through the grid for (t_0 − 120 h) (m s^{-1}). (b) As in (a), except for t_0 + 120 h.

noted for meridional shears.) Fig. 17 taken from their paper shows composites of zonal shear for WI non-developing cloud clusters and pre-hurricane clusters and depressions, with the grid centered on the system. The non-developing clusters show a weak gradient of shear with positive values over the storm, while the pre-hurricane systems exhibit strong meridional gradients of vertical shear and zero shear over the system. Fig. 18a, b, shows plan views of vertical shear of the zonal wind 120 h before and 120 h after hurricane passage. The flow changes from an unfavorable shear pattern for cyclogenesis 120 h prior to passage to a favorable pattern persisting 120 h after passage. Similar changes are observed from 60 h before to 60 h after storm passage.

Fig. 19 shows vertical shear of the zonal wind for WPAC non-developing clusters and pre-typhoon clusters from McBride and Zehr. The developing systems are associated with a zero shear line running through their centers and stronger north–south gradients of the shear. Fig. 20a, b, shows plan views of the shear 120 h before and 120 h after typhoon passage (±60 h are similar to ±120 h). The pattern differs from the WI (Fig. 18) in that conditions are favorable both prior to and after passage. The reason for the difference is the presence of the extensive upper-level southwest outflow channel in typhoons. As shown in Figs. 12–14, the average typhoon has a significant "upstream" influence on the large-scale flow while the mean hurricane does not.

Figs. 18 and 20 suggest that the large-scale vorticity patterns are favorable for tropical cyclogenesis in the wakes of westerly-moving hurricanes and typhoons and in the path areas ahead of the typhoons. However, McBride and Zehr (1981) showed that tropical cyclones form from convective systems with

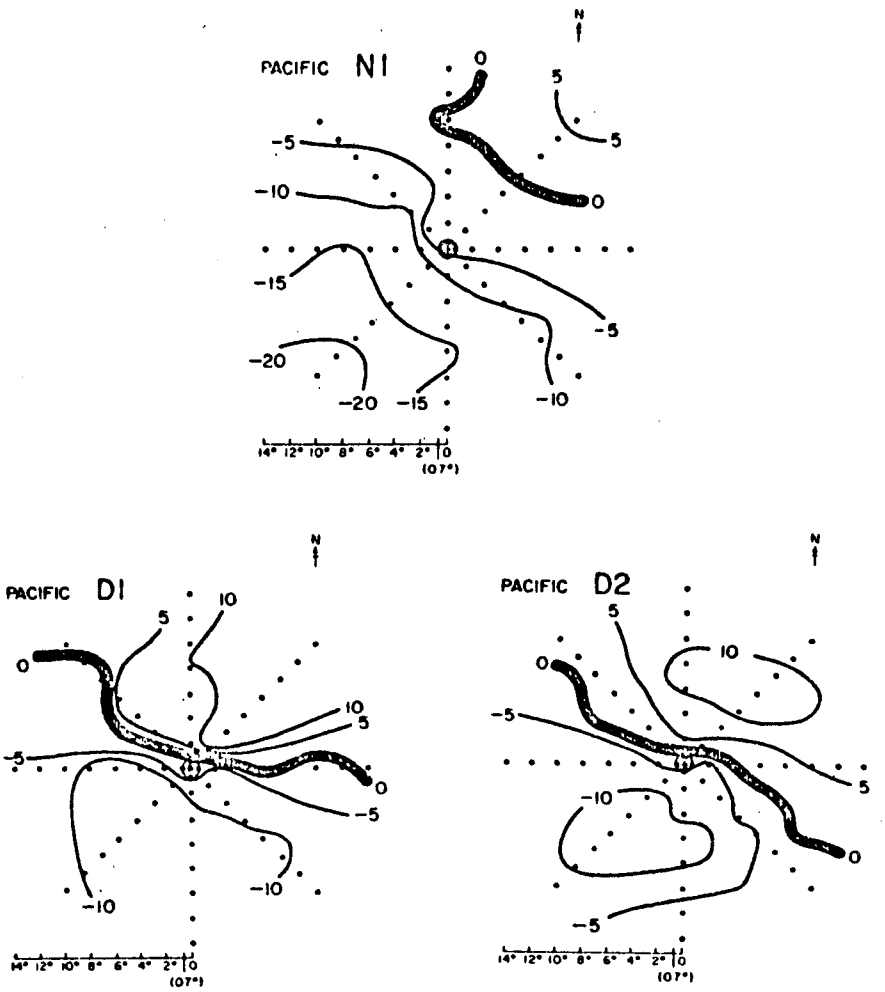

FIG. 19. Vertical shear of the zonal wind as in Fig. 17 for WPAC non-developing clusters (N1), early pre-typhoon (D1), and pre-typhoon clusters (D2) from McBride and Zehr (1981) (m s^{-1}).

significant upward mean vertical motions. Fig. 15 showed that the path area ahead of the typhoon exhibits subsidence and is therefore suppressed while the wake exhibits large-scale upward vertical motion. Combining the effects of the rotational and divergent flow it is seen that the wake regions of both cyclones appear favorable for cyclogenesis while the path regions do not. Examining the total data set, Fig. 21 shows the locations of the existing typhoons (1957–77) relative to the center positions of new storms at the times when the latter first strengthened to typhoon intensity. The mean track direction is toward the northwest. Of the 56 total existing storms within 40° east and west of the new typhoons, 38 were west of the new storms and only 18 were to the east. The existing storms were most commonly found near points ±15–20° longitude from the new storm and at approximately the same latitude. When assessing Fig. 21 it should be noted that a pattern of this kind could also occur if large-scale circulation features often create local regions favorable for cyclone intensification which tend to persist in time and space for ~5 days or more—an area for future study.

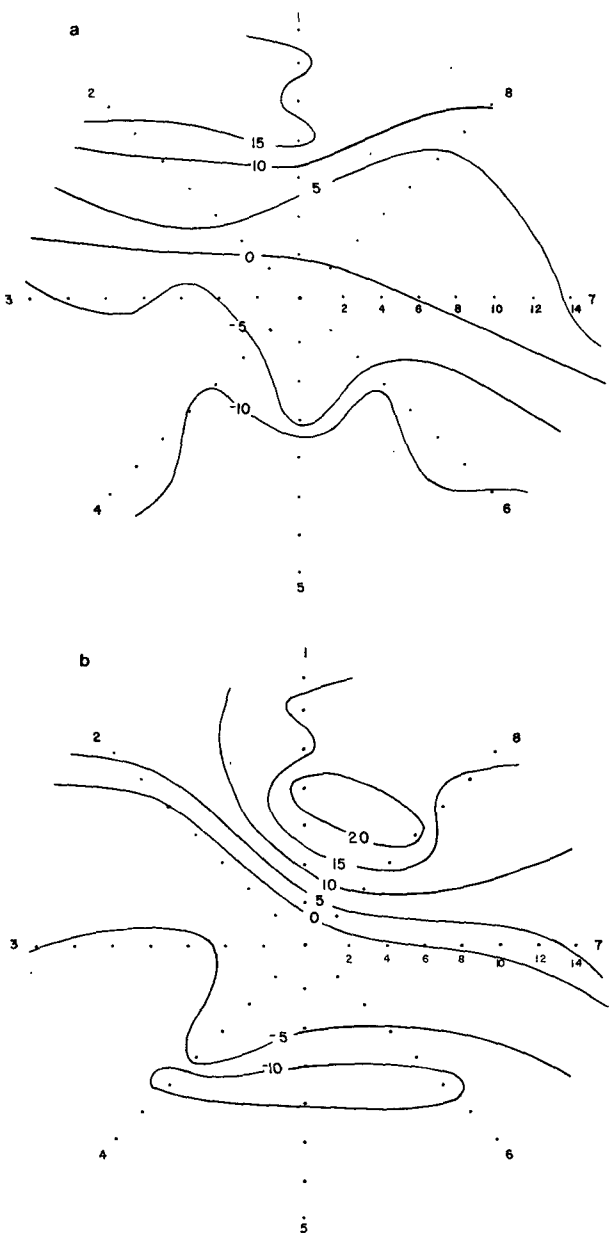

FIG. 20. Plan view of vertical shear of the zonal wind (U at 200 mb minus U at 900 mb) 120 h prior to the passage of a typhoon through the grid (t_0 − 120 h) (m s^{-1}). (b) As in (a), except for t_0 + 120 h.

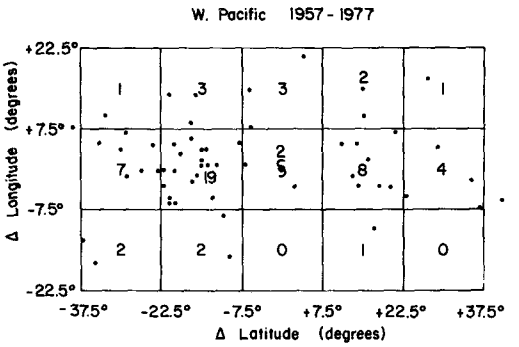

FIG. 21. Locations of previously existing typhoons relative to the positions of new storms when they first reach typhoon intensity. Data set is all WPAC typhoons from 1957–1977. Numbers denote totals in 15 × 15° latitude squares.

The storms used in the storm passage analyses were all on west to northwesterly tracks. Therefore, the mean path is generally west of the storm while the wake is to the east. It may be that the above relationships regarding large-scale storm effects on subsequent cyclogenesis pertain to geographical positioning relative to the storm as well as to position relative to storm direction of motion.

4. Conclusions

The influences and circulations of tropical cyclones are shown to extend large distances from the intense central cores. At large radii the flow is predominantly anticyclonic and is strongest in the upper troposphere. The strength of the tangential circulation at large radii increases with increasing strength of the core. However, the convergence and vertical motion changes which occur as the storms intensify from prestorm disturbances to mature systems are confined to the inner 6° and 2° radius, respectively. The storms have outflow channels usually located in the northeast (typhoons and hurricanes) and southwest (typhoons only) quadrants which extend past the 15° limit of the grid in the case of the Pacific systems.

Mature tropical cyclones act as significant large-

scale sources of kinetic energy and sinks of relative angular momentum. West Pacific typhoons make a small contribution to the poleward flux of kinetic energy and westerly momentum, and both hurricanes and typhoons contribute to the kinetic energy of the tropical latitudes. The passage of both typhoons and hurricanes resulted in substantial increases in large-scale kinetic energy over a 10-day period. The radial exports and meridional fluxes of kinetic energy and momentum were the only processes studied which were significantly related to the strength of the storm core, and even these appeared to be related to the large-scale structure of the upper-level anticyclone. It is doubtful whether changes of core strength would affect these large-scale fluxes unless the entire upper-level circulation were to weaken as well.

From a large-scale thermodynamic viewpoint all of the systems studied were nearly self-contained. Although the systems did act to converge moisture and diverge dry and moist static energy through 12° radius, these fluxes were relatively small and bore little relation to the intensity of the system.

The path regions ahead of westerly-moving typhoons show increased upper level anticyclonic rotation and suppressed vertical motion (subsidence) up to five days prior to the storm arrival, in agreement with satellite observations of frequent large clear areas to the northwest of typhoons. Both the hurricane and typhoon wake regions exhibit increased upper-level anticyclonic flow and upward vertical motion, with the hurricane wake anomaly extending through 60 h and the typhoon through 120 h following storm passage. Based on current tropical cyclogenesis criteria, the wake regions of west to northwesterly moving tropical cyclones appear to be enhanced areas for cyclogenesis. The path regions of these typhoons are generally less favorable for cyclogenesis. Typhoons are found to be twice as likely to develop to the east of existing typhoons as they are to develop to the west.

Acknowledgments. The author wishes to express his sincere gratitude to Prof. William Gray and Mr. Edwin Buzzell of Colorado State University for performing the composite computer runs and to Miss Mary Morris for her preparation of the manuscript. This research was supported by NOAA under contract NA80RAA-00271 and a grant from the National Science Foundation ATM79-05677.

REFERENCES

Black, P. G., and R. A. Anthes, 1971: On the asymmetric structure of the tropical cyclone outflow layer. *J. Atmos. Sci.*, **28,** 1348–1366.

Edmon, H. J., Jr., and D. G. Vincent, 1979: Large-scale conditions during the intensification of Hurricane Carmen (1974). II. Diabatic heating rates and energy budget. *Mon. Wea. Rev.*, **107,** 295–313.

Erickson, C. O., and J. S. Winston, 1972: Tropical storm midlatitude cloud-band connections and the autumnal build-up of the planetary circulation. *J. Appl. Meteor.*, **11,** 23–36.

Frank, W. M., 1976: The structure and energetics of the tropical cyclone. Atmos. Sci. Pap. No. 258, Colorado State University, 180 pp. [NTIS 263152.]

——, 1977a: The structure and energetics of the tropical cyclone, Part I: Storm structure. *Mon. Wea. Rev.*, **105,** 1119–1135.

——, 1977b: The structure and energetics of the tropical cyclone, Part II: Dynamics and energetics. *Mon. Wea. Rev.*, **105,** 1136–1150.

——, 1977c: Convective fluxes in tropical cyclones. *J. Atmos. Sci.*, **34,** 1554–1568.

Gray, W. M., 1975: Tropical cyclone genesis. Atmos. Sci. Pap. No. 243, Colorado State University, 119 pp.

——, 1978: Hurricanes: their formation, structure and likely role in the tropical circulation. *Proc. Joint Conf. Meteorology over the Tropical Oceans*, London, Roy. Meteor. Soc., Amer. Meteor. Soc., Deutsche Meteor. Gesellsch., 155–218.

McBride, J. L., 1979: Observational analysis of tropical cyclone formation. Colorado State University, Atmos. Sci. Pap. No. 308, 230 pp. [NTIS 80-133614.]

——, 1981a: Observational analysis of tropical cyclone formation, Part I: Basic description of data sets. *J. Atmos. Sci.*, **38,** 1117–1131.

——, 1981b: Observational analysis of tropical cyclone formation, Part II: Budget analysis. *J. Atmos. Sci.*, **38,** 1152–1166.

——, and R. Zehr, 1981: Observational analysis of tropical cyclone formation, Part II: Comparison of non-developing versus developing systems. *J. Atmos. Sci.*, **38,** 1132–1151.

Miller, B. I., 1958: The three-dimensional wind structure around a tropical cyclone. Nat. Hurricane Res. Proj., Rep. No. 15, 41 pp. [Available from the National Hurricane Research Laboratory, Miami, FL.]

Newell, R. E., J. W. Kidson, D. G. Vincent and G. J. Boer, 1972: *The General Circulation of the Tropical Atmosphere and Interactions with Extratropical Latitudes.* MIT Press, 258 pp.

Nunez, E., and W. M. Gray, 1977: A comparison between West Indies hurricanes and Pacific typhoons. *Proc. 11th Tech. Conf. on Hurricanes and Tropical Meteorology*, Miami, Amer. Meteor. Soc., 528–534.

Ooyama, K., 1969: Numerical simulation of the life cycle of tropical cyclones. *J. Atmos. Sci.*, **26,** 3–40.

Palmén, E. H., 1958: Vertical circulation and release of kinetic energy during the development of Hurricane Hazel into an extratropical storm. *Tellus*, **10,** 1–23.

Reed, R. J., and E. E. Recker, 1971: Structure and properties of synoptic scale wave disturbances in the equatorial eastern Pacific. *J. Atmos. Sci.*, **28,** 1117–1133.

——, D. C. Norquist and E. E. Recker, 1977: The structure and properties of African wave disturbances as observed during Phase III of GATE. *Mon. Wea. Rev.*, **105,** 317–333.

Rodgers, E. B., and R. F. Adler, 1981: Tropical cyclone rainfall characteristics as determined from a satellite passive microwave radiometer. *Mon. Wea. Rev.*, **109,** 506–521.

Rosenthal, S., 1970: A circularly symmetric primitive equation model of tropical cyclone development containing an explicit water vapor cycle. *Mon. Wea. Rev.*, **98,** 643–663.

Shapiro, L. J., 1977: Tropical storm formation from easterly waves: a criterion for development. *J. Atmos. Sci.*, **34,** 1007–1021.

Shea, D. J., and W. M. Gray, 1973: The hurricane's inner core region. I. Symmetric and asymmetric structure. II. Thermal stability and dynamic characteristics. *J. Atmos. Sci.*, **30,** 1544–1564 and 1565–1576.

Vincent, D. G., and R. G. Waterman, 1979: Large-scale atmospheric conditions during the intensification of Hurricane Carmen (1974). I. Temperature, moisture and kinematics. *Mon. Wea. Rev.*, **107,** 283–294.

Williams, K. T., and W. M. Gray, 1973: Statistical analysis of satellite observed cloud clusters in the western North Pacific. *Tellus*, **25,** 178–201.